The 20.5th Cambridge Workshop on Cool Stars, Stellar Systems, and the Sun
Edited by S. J. Wolk, A. K. Dupree, H. M. Günther

Chromospheric activity to age relationship among Sun-like stars

Philippe Gondoin

Abstract

The emission reversal in the cores of the CaII H&K lines of late-type dwarfs is correlated with their age and is potentially an accurate age indicator. Recent measurements of stellar rotation periods in intermediate-age open clusters indicate that the rotation rates of Sun-like stars older than 1 Gyr decay as age$^{0.49M-1.19}$ for stellar masses M included between 0.7 and 1.1 M$\odot$. The corresponding evolution of the $R^{'}_{\rm HK}$ activity index inferred from rotation-activity relationships is steeper than the relationship $R^{'}_{\rm HK} \propto$ age$^{-0.5}$ generally used. Such a steep decay of the chromospheric activity beyond the age of 1 Gyr is supported by measurements of the $R^{'}_{\rm HK}$ index distributions among nearby G and K main sequence stars with near solar metallicity.

1 Introduction

It has long been known that the emission reversal in the cores of the CaII H&K Fraunhofer lines of late-type dwarfs is correlated with their age and is potentially an accurate age indicator (e.g. Wielen 1974). The emission in the cores of the CaII H&K lines is a well-known sign of departure from radiative equilibrium that requires additional mechanisms that are generally termed activity (Hall 2008). A major contributor to stellar activity is the evolution and variability of magnetic fields via heating by Alfvén waves or transport of mechanical energy along magnetic flux tubes into the outer atmosphere of cool stars.

Because of various uncertainties in observational data, Mayor & Martinet (1977) could not significantly constrain the time variation of the stellar birth rate in the solar neighbourhood from the kinematics and calcium emission intensity of nearby K dwarfs. Several studies have intended to calibrate this emission as a function of age (e.g. Skumanich 1972, Soderblom et al. 1991, Lachaume et al. 1999). Although some controversy arose on the use of chromospheric emission as a reliable age indicator (Pace 2013), recent studies have confirmed the viability of deriving usable chromospheric ages for solar-type stars up to at least 6 Gyr, providing that mass and metallicity effects are accounted for (Lorenzo-Oliveira et al. 2016).

The chromospheric activity level of cool stars has traditionally been quantified by the $R^{'}_{\rm HK}$ index, defined as the ratio of the emission in the core of the CaII H&K lines to the total bolometric emission of the star (Noyes et al. 1984). This index can be expressed as follows:

$$R^{'}_{\rm HK} = \frac{F^{'}_{\rm H} + F^{'}_{\rm K}}{\sigma T^{4}_{\rm eff}} \quad (1)$$

where $F^{'}_{\rm H}$ and $F^{'}_{\rm K}$ are the emission fluxes in the cores of the CaII H&K lines and σ is the Stefan-Boltzmann constant.

Using high resolution spectroscopic observations of a large sample of solar twins, Lorenzo-Oliveira et al. (2018) derived a relationship $R^{'}_{\rm HK} \propto Age^{-0.52}$ valid for solar twins with ages between 0.6 and 9 Gyr, which they interpreted as an approximation of the more complex activity evolution relationship formulated by Mamajek & Hillenbrand (2008). Some scatter was attributed to stellar cycle modulation effects. Using a sample of solar-type stars with asteroseismic ages, Booth et al. (2019) also find a reasonable agreement with the Mamajek & Hillenbrand (2008) relationship, with some scatter due to stellar mass.

The dependence of magnetic activity on stellar mass and age renders a direct measurement of the magnetic activity evolution difficult. In addition, the long-term evolutionary trend of activity indicators is blurred by the short-time variability of magnetic phenomena that includes the evolution of active regions and activity cycles. The determination of an average magnetic activity level at different ages thus requires observations of large numbers of coeval stars. Such samples are found in open clusters but their observations generally lead to incomplete measurements. Those are limited by the low brightnesses of activity indicators in weakly or moderately active stars and by the large distances of clusters. An alternative approach is to measure activity indices on a large number of field stars but their ages are seldom known to sufficient accuracy.

In order to overcome these difficulties, I characterised the long-term evolution of chromospheric activity on Sun-like stars indirectly, following the approach used in Gondoin (2018, 2020a). The approach consists of combining a best fit parametric model of the rotation evolution of Sun-like stars in open clusters with rotation-activity relationships.

2 Stellar rotation in open clusters

Photometric surveys of open clusters (see e.g. Affer et al. 2013; Delorme et al. 2011; Hartman et al. 2010; Irwin et al. 2009; Meibom et al. 2011) have produced extensive rotation period measurements on Sun-like stars of different ages. These results have been used to test angular momentum evolution models (e.g., MacGregor & Charbonneau 1995; Dennissenkov et al. 2010; Reiners & Mohanty 2012; Gondoin 2017). This approach implicitly assumes that the distributions of rotation periods among Sun-like stars in open clusters of various ages result from the evolution of similar

Table 1: Mean rotation periods (in days) vs mass and age of main-sequence stars with near-solar metallicity derived from measurements in NGC 6811 (Meibom et al. 2011; Curtis et al. 2019), NGC 6819 (Meibom et al. 2015), and M67 (Barnes et al. 2016).

	Age (Gyr)		
$M/M_\odot$	1.0	2.4	4.0
0.7	12.0		36.0
0.8	10.6	23.2	31.5
0.9	11.0	21.6	29.0
1.0	10.6	18.2	25.8
1.1	8.7	15.2	21.3

initial distributions of rotation periods after dispersion of circumstellar disks. Such an assumption is justified by the fact that Sun-like stars in open clusters that have similar ages also show similar distributions of rotation periods and activity levels (e.g. Fritzewski et al. 2020).

Those extensive measurements of rotation periods show a bimodal distribution of stellar rotation in young open clusters (e.g., Barnes 2003; Meibom et al. 2011). Young Sun-like stars tend to group into two distinct populations of fast and slow rotators. These populations lie on narrow sequences in diagrams where the measured rotation periods of the members of a stellar cluster are plotted against their B − V colors. Beyond the age of approximately ∼600 Myrs, the two populations converge towards a unique sequence of slow rotators. The rotation period of their stellar members can then be unambiguously parametrised as a function of age, mass, and metallicity.

The evolution of the mean rotation rates of Sun-like stars beyond 1 Gyr can thus be derived from measured rotation periods versus $B-V$ indices or effective temperatures in NGC 6811 (Meibom et al. 2011; Curtis et al. 2019), NGC 6819 (Meibom et al. 2015), and M67 (Barnes et al. 2016). These clusters are 1.0 Gyr (Sandquist et al. 2016), 2.4 Gyr (Brewer et al. 2016), and 4 Gyr (VandenBerg et al. 2004) old, respectively, and have solar metallicities (Corsaro et al. 2017, Liu et al. 2019). The $B-V$ indices and effective temperatures of their stellar members can be converted to masses based on a survey of the literature and catalogue values. The mean rotation periods versus masses and ages inferred from measurements in those open clusters are summarised in Table 1.

Based on this information, Gondoin (2020b) derived a formulation of the rotation periods of 0.7 to 1.1 $M_\odot$ main-sequence stars with near-solar metallicity as a function of their mass and age that is valid between the ages of 1 and 4 Gyr, that is to say:

$$P(t,M) = P(t_0,M) \times (t/t_0)^{(1.19-0.49M)} \quad (2)$$

where $P(t_0,M)$ = 179.36-576.4M +654.52M^2 -247.1M^3 and t_0 = 1 Gyr. P is the rotation period of the star in days, M is its mass in solar unit, and t is its age in Gyr. The exponent of the powerlaw relationship is a uniformly decreasing function of mass that is significantly higher than the 0.5 value most often used. Figure 1 (left) shows the interpolated evolution of the rotation periods of 0.7, 0.8, 0.9, 1.0, and 1.1 $M_\odot$ stars between the ages of 1 and 4 Gyr. This evolution depends on stellar mass with a steeper decay of the rotation rate for low-mass stars.

3 Empirical rotation-activity relationship

Stellar activity is closely related to rotation and its interplay with convection. Pallavicini et al. (1981) first found a correlation between the X-ray luminosities and projected rotational velocities of G to M stars including giants and binary stars. Mangeney and Praderie (1984) suggested that the convection-rotation interaction is better represented by an effective Rossby number that measures the efficiency of rotation in inducing helicity and differential rotation (Durney & Latour 1978). This stellar-mass dependent parameter has been used to minimise the scatter due to mass in many studies of correlations between rotation and activity. Empirical rotation-activity relationships have been obtained for stars with different masses, rotation periods, and activity levels.

In particular, Mamajek & Hillenbrand (2008) derived a biunique relationship between the chromospheric activity index $R^{'}_{\rm HK}$ of main-sequence stars and their Rossby number, that is to say:

$$\log R^{'}_{\rm HK} = \begin{cases} -4.35 - 1.451({\rm Ro} - 0.32) & \text{if Ro} < 0.32 \\ -4.35 - 0.337({\rm Ro} - 0.32) & \text{if Ro} \geq 0.32 \end{cases} \quad (3)$$

where the Rossby number Ro is defined as the ratio of the star's rotation period P over its convective turnover time $\tau_{\rm conv}$. Here P is time and mass dependent while $\tau_{\rm conv}$ mainly depends on stellar mass for main-sequence stars (e.g. Landin et al. 2010), hence:

$$\text{Ro(t,M)} = \text{P(t, M)}/\tau_{\rm conv}(M) \quad (4)$$

Equation 4 uses the Rossby number values derived from the convective turnover time relation as a function of $B-V$ colour that was established empirically by Noyes et al. (1984). This determination has often been used in the literature, although it was initially based on only a few points redder than $B-V=1.0$. Pizzolato et al. (2003) provided improved values using a sample with a greater coverage of low-mass stars. Based on these consolidated values, Wright et al. (2011) suggest that stellar mass is the relevant physical parameter that determines the convective turnover time and derived the following relationship:

$$\log(\tau_{\rm conv}) = 1.16 - 1.49 \times \log(M) - 0.54 \times \log^2(M) \quad (5)$$

where M is the mass in solar unit. This relationship is valid over the range $0.09 < M < 1.36$. It is in good agreement (see Fig. 7 in Wright et al. 2011) with that of Noyes et al. (1984).

4 Inferred activity to age relationship

I used the empirical formulation of the convective turnover time by Wright et al. (2011) and derived the long-term evolution of the $R^{'}_{\rm HK}$ index of main-sequence stars with masses between 0.7 $M_\odot$ and 1.1 $M_\odot$ combining Eqs. 2, 3, 4, and 5. In the absence of rotation period measurements in open clusters older than 4 Gyr, this empirical derivation of $R^{'}_{\rm HK}$ becomes uncertain beyond the age of the Sun. However, beyond this age, observations of field stars show that the emission flux in the cores of the CaII H&K lines reaches a lower limit, the so-called basal chromospheric flux (Schrijver 1987). The basal chromospheric flux appears not to be photospheric

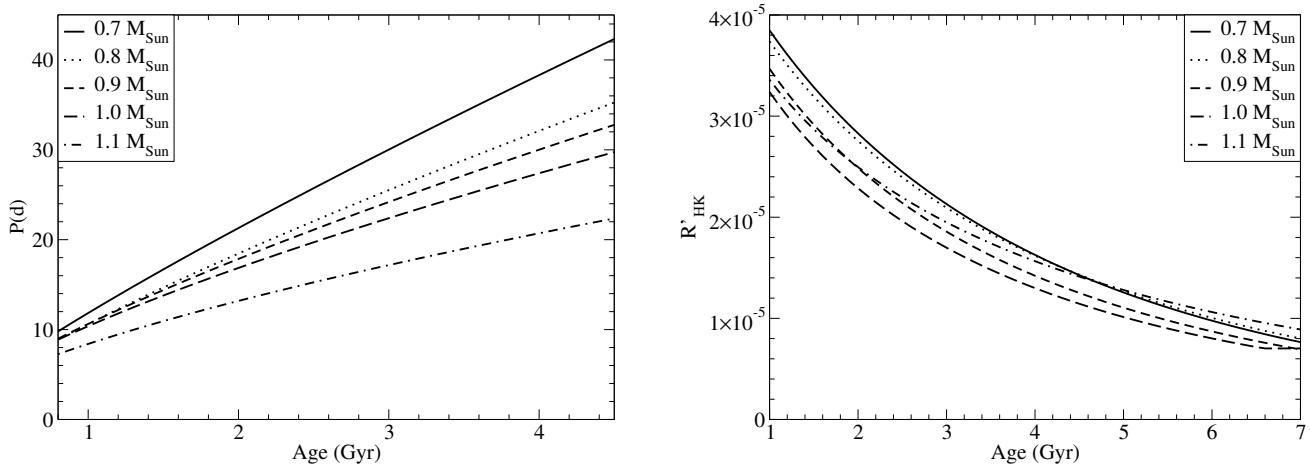

Figure 1: Left: rotation period evolution of 0.7-1.1 $M_\odot$ stars with near-solar metallicity derived from rotation period measurements in NGC 6811 (1 Gyr; Curtis et al. 2019), NGC 6819 (2.4 Gyr; Meibom et al. 2015), and M67 (4.0 Gyr; Barnes et al. 2016). Right: average Ca II $R^{'}_{\rm HK}$ index of 0.7 to 1.1 $M_\odot$ stars derived from the long-term evolution of their rotation period.

in nature but rather reflects a residual chromospheric heating. It could either result from the dissipation of mechanical, not magnetic, wave energy such as acoustic waves (e.g. Perez-Martinez et al. 2011 and references therein) or from the action of a minimal magnetic activity.

This empirical limit distinctly depends on effective temperature (Rutten et al. 1991). Using the empirical formula of Perez Martinez et al. (2014) for the basal Ca II flux as a function of the star effective temperature $T_{\rm eff}$, the corresponding basal chromospheric activity index $R^{'\rm bas}_{\rm HK}$ can be expressed as follows:

$$\log(R^{'\rm bas}_{\rm HK}) = 3.05 \times \log(T_{\rm eff}) - 16.61 \qquad (6)$$

To limit the uncertainty on the chromospheric activity level of stars older than 4 Gyr, I calculated the $R^{'}_{\rm HK}$ index evolution of 0.7-1.1 $M_\odot$ stars using Eq. 3 until it reaches the mass dependent basal chromospheric index $R^{'\rm bas}_{\rm HK}$. I then assumed that $R^{'}_{\rm HK}$ remains constant to this value. According to this model, a solar-mass star would reach the basal chromospheric activity level at an age of ∼6.6 Gyr. However, recent data from Booth et al. (2020) indicate that magnetic activity continues to decrease even at old stellar ages for both G-type stars and the coolest F-type stars that have a convective envelope.

While stellar rotation evolves slowly with time, magnetic activity varies on much shorter timescales. The physical mechanisms producing such variability include changes in the filling factor of active regions, growth and decay of individual emitting regions, and activity cycles. I used the results from Radick et al. (1998) to estimate the dispersion of the $R^{'}_{\rm HK}$ indices due to the short-term variability of magnetic activity around the average $< R^{'}_{\rm HK} >$ values derived from the long-term evolution of stellar rotation. The authors found that chromospheric variations for their entire sample of F5- to K7-type stars that spanned a range of chromospheric activity indices between -5.05 and -4.15 were fairly well related by power laws to average chromospheric activity levels. An estimate of the cyclic chromospheric RMS variation (see Fig. 5 in Radick et al. 1998) is given by:

$$\mathrm{RMS}(< R^{'}_{\rm HK} >) = 0.327 \times < R^{'}_{\rm HK} >^{1.15} \qquad (7)$$

The right-hand graph in Fig. 1 shows the derived evolutions of the $R^{'}_{\rm HK}$ index for 0.7, 0.8, 0.9, 1.0, and 1.1 $M_\odot$ dwarfs, excluding the short-term variability of their magnetic activity. The curves are remarkably similar, indicating that the chromospheric activity to age relationship depends moderately on mass in the 0.7 to 1.1 $M_\odot$ range. The $R^{'}_{\rm HK}$ indices of 0.7-0.8 $M_\odot$ stars decay slightly faster than those of 1.0-1.1 $M_\odot$ stars. Solar-mass stars reach their basal chromospheric level around the age of 7 Gyr, while lower-mass stars reach their lowest activity level later, beyond the age of 10 Gyr for 0.7 $M_\odot$ stars.

In the 0.7 to 1.1 $M_\odot$ range, the relative dispersion of the $R^{'}_{\rm HK}$ index resulting from the short-term variability of chromospheric activity is about 6 to 7 %, according to Eq. 7. Its relative variation due to mass is ∼9% at 1 Gyr and 11% at 4 Gyr (see right-hand graph in Fig. 1).

5 Discussion

The magnetic activity of Sun-like stars younger than about ∼600 Myr depends not only on their mass and age but also on their initial rotation rate after circumstellar disc dispersion (Gondoin 2018). Beyond ∼600 Myr, the rotation rates of Sun-like stars with similar masses converge towards similar values (e.g. Gondoin 2017 and reference therein) and stellar age becomes the main parameter that determines the chromospheric activity level of 0.7-1.1 $M_\odot$ stars with near-solar metallicity (see Fig. 1, right). Beyond the age of ∼6 or 7 Gyr, the chromospheric activity of old Sun-like stars gets close to its basal chromospheric activity level and barely decays with age. The distribution of $R^{'}_{\rm HK}$ indices in a population of Sun-like stars with near-solar metallicity can thus be used to constrain its age distribution between about 0.6 and 6 Gyr.

Following the approach in Gondoin (2018, 2020a), I derived

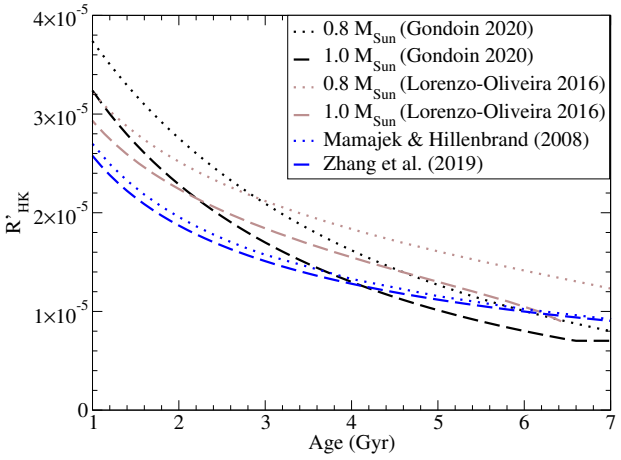

Figure 2: Average Ca II $R^{'}_{\rm HK}$ index evolution of 0.8 to 1.0 $M_{\odot}$ stars with near-solar metallicity derived from their rotation period evolution compared with previous studies. These include (i) the relationship of Lorenzo-Oliveira et al.(2018) for 0.8 and 1.0 $M_{\odot}$ stars with solar metallicity, (ii) the age-activity relationships of Mamajek & Hillenbrand (2008) for F7-K2 dwarfs ($0.5 < B-V < 0.9$), and (iii) the age-activity relationship of Zhang et al.(2019) for stars with 4000 K $< T_{\rm eff} <$ 5500 K.

a model of the $R^{'}_{\rm HK}$ index evolution of 0.7-1.1 $M_{\odot}$ stars combining a rotation-activity relationship with available rotation period measurements in intermediate-age open clusters, namely NGC 6811, NGC 6819, and M67 that are 1.0, 2.4, and 4.0 Gyr old, respectively. Figure 2 compares this evolution for 0.8 and 1.0 $M_{\odot}$ dwarfs with the age versus $R^{'}_{\rm HK}$ relationship from Lorenzo-Oliveira et al. (2018) applied to 0.8 and 1.0 $M_{\odot}$ stars with a solar metallicity. This relationship was derived from a sample of field stars selected from Adibekyan et al. (2012) and complemented with selected objects from the Pleiades (0.1 Gyr), the Ursa Major (0.3 Gyr) moving group, the Hyades (0.6 Gyr), and M67 (4.0 Gyr). The $R^{'}_{\rm HK}$ versus age relationship that I derived from rotation period measurements in clusters is similar to, though steeper than, the relationship from Lorenzo-Oliveira et al. (2018). For 0.8 and 1.0 $M_{\odot}$ dwarfs, the $R^{'}_{\rm HK}$ versus age curves of the two studies intercept each other at ages of 2.8 and 2.2 Gyr, respectively.

Figure 2 also compares the evolution of the $R^{'}_{\rm HK}$ activity index that I derived from rotation period measurements in NGC 6811, NGC 6819, and M67 with the mean $R^{'}_{\rm HK}$ age relationship from Mamajek and Hillenbrand (2008). The $R^{'}_{\rm HK}$ decay inferred from rotation period measurements in the intermediate-age clusters is also steeper than the $R^{'}_{\rm HK}$ decay derived by Mamajek and Hillenbrand (2008) from $R^{'}_{\rm HK}$ data in young (< 0.7 Gyr) open clusters and in M67 (4 Gyr). Figure 2 also shows the $R^{'}_{\rm HK}$ to age relationship derived from Zhang et al. (2019; see their Fig. 9a) for stars with 4000 K $<$ T$_{\rm eff}$ $<$ 5000 K, assuming $R^{'}_{\rm HK} = 2 \times R^{'}_{\rm K}$, where $R^{'}_{\rm K}$ is the emission in the Ca II H&K line normalised to the photospheric flux. The obtained relationship is similar to the one in Mamajek and Hillenbrand (2008). It is the result of a quadratic fit to the average $R^{'}_{\rm K}$ index in 22 open clusters, of which 20 are younger than 1 Gyr.

The origin of the difference between the $R^{'}_{\rm HK}$ versus age relationship derived from rotation period measurements in intermediate-age open clusters and previous studies comes from recent observations that stars experience a reduced braking efficiency and stalled spin-down between the ages of ∼670 Myr and ∼1 Gyr (Curtis et al. 2019; Spada & Lanzafame 2020). Since activity is closely related to rotation, a decay of the chromospheric activity should only begin when stars approach an age of ∼1 Gyr. The decay of the $R^{'}_{\rm HK}$ index inferred from rotation period measurements in 1.0, 2.4, and 4.0 Gyr old clusters is thus steeper than the activity evolution derived from best fits to measured $R^{'}_{\rm HK}$ data in young (< 0.7 Gyr) open clusters and in M67 (∼4 Gyr).

Gondoin (2020b) used this steeper model of chromospheric activity evolution to retrieve the age distributions of parent populations of nearby Sun-like stars in the thin and thick discs of the Galaxy. The Monte Carlo analysis based on this model indicates that the measured $R^{'}_{\rm HK}$ index distributions among 0.7-1.1 $M_{\odot}$ stars from the thin disc can be explained by a combination of old (> 6-7 Gyr) star formation events and a more recent burst of star formation that started ∼2.3 Gyr ago. This conclusion is consistent with photometric, astrometric, and archaeo-chemistry studies that report a recent burst of a star formation that occurred 2-3 Gyr ago in the Galactic thin disc domain.

6 Conclusion

Measurements of stellar rotation in intermediate-age open clusters indicate that the rotation rate of Sun-like stars older than1 Gyr decays as age$^{0.49M-1.19}$ for stellar masses M between 0.7 and 1.1 M$\odot$. The corresponding evolution of the $R^{'}_{\rm HK}$ activity index inferred from rotation-activity relationships is steeper than the relationship R$^{'}_{\rm HK}$ $\propto$ age$^{-0.5}$ generally used. Such a steep decay of the chromospheric activity beyond 1 Gyr is supported by measurements of the $R^{'}_{\rm HK}$ index distributions among nearby G and K main sequence stars with a near-solar metallicity.

Acknowledgments

I am grateful to the organising committee of the Cool Stars 20.5 workshop for allowing me to present this work.

References

Adibekyan, V. Zh., Sousa, S. G., Santos, N. C. et al. 2012, A&A, 545, A32
Affer, L., Micela, G., Favata, F. et al. 2013, MNRAS, 430, 1433
Barnes, S. A. 2003, ApJ, 586, 464
Barnes, S. A., Weingrill, J., Fritzweski, D., et al. 2016, ApJ, 823, 16
Booth, R. S., Poppenhaeger, K., Watson, C. A. et al. 2020, MNRAS, 491, 455
Brewer, L.N., Sandquist, E.L., Mathieu, R.D., et al. 2016, ApJ, 151, 66
Corsaro, E., Mathur, S., Garcia, R. A. et al. 2017, A&A, 605, A3
Curtis, J. L., Agueros, M. A., Douglas, S. T. et al. 2019, ApJ, 879, 49

Delorme, P., Collier Cameron, A., Hebb, L. et al. 2011, MNRAS, 413, 2218
Denissenkov, P. A., Pinsonneault, M., Terndrup, D.M., & Newsham, G. 2010, ApJ, 716, 1269
Durney, B. R., Latour, J. 1978, Geophys. and Astrophys. Fluid Dyn., 9, 241
Fritzewski D. J. , Barnes S.A., James D.J., & Strassmeier K. G. 2020, A&A, 641, A51
Gondoin, P. 2017, A&A, 599, A122
Gondoin, P. 2018, A&A, 616, A154
Gondoin, P. 2020a, AN, 341, Issue 5, pp. 557-566
Gondoin, P. 2020b, A&A, 641, A110
Hall, J.C. 2008, Living Rev. Solar Phys., 5, 2
Hartman, J. D., Bakos, G. Á., Kovács, G., & Noyes, R. W. 2010, MNRAS, 408, 475
Irwin, J., Aigrain, S., Bouvier, J. et al. 2009, MNRAS, 392, 1456
Lachaume, R., Dominik, C., Lanz, T. et al. 1999, A&A, 348, 897
Landin, N. R., Mendes, L. T. S., & Vaz, L. P. R. 2010, A&A, 510, A46
Liu, F., Asplund, M., Yong, D. et al. 2019, A&A, 627, A117
Lorenzo-Oliveira, D., Porto de Mello, G. F., & Schiavon, R. P. 2016, A&A, 594, L3
Lorenzo-Oliveira, D., Freitas, F. C., Melendez, J. et al. 2018, A&A, 619, A73
MacGregor, K. B., & Charbonneau, P. 1995, Cool Stars; Stellar Systems; and the Sun; Eighth Cambridge Workshop. Astronomical Society of the Pacific Conference Series, Vol. 64, p.174
Mamajek, E. E., & Hillenbrand, L. A. 2008, ApJ, 687, 1264
Mangeney, A., & Praderie, F. 1984, A&A, 130, 143
Mayor, M., & Martinet, L. 1977, A&A, 55, 221
Meibom, S., Barnes, S. A., Latham, D. W. et al. 2011, ApJ, 733, L9
Meibom, S., Barnes, S.A.., Platais, I. et al. 2015, Nature, 517, 589
Noyes, R. W., Hartmann, L. W., Baliunas, S. L. et al. 1984, ApJ, 279, 763
Pace, G. 2013, A&A, 551, L8
Pallavicini, R., Golub, L., Rosner, R., et al. 1981, ApJ, 248, 279
Perez Martinez, M. I., Schroder, K.-P., & Hauschildt 2014, MNRAS, 445, 270
Pizzolato, N., Maggio, A., Micela, G., Sciortino, S., & Ventura, P. 2003, A&A, 397, 147
Radick, R. R., Lockwood, G. W., Skif, B.A., & Baliunas, S. L. 1998, ApJS, 118, 239
Reiners, A. & Mohanty S. 2012, ApJ, 746, 43
Sandquist, E.L., Jessen-Hansen, J., Shetrone, M.D. et al. 2016, ApJ, 831, 11
Schrijver, C. J. 1987, A&A, 172, 111
Skumanich, A. 1965, AJ, 70, 692
Soderblom, D. R., Duncan, D. K., & Johnson, D. R. H. 1991, ApJ, 375, 722
Spada, F., & Lanzafame A. C. 2020, A&A, 636, A76
VandenBerg, D.A., Don, A., & Stetson, P.B. 2004, PASP, 116, 997
Wielen, R. 1974 in Highlights of Astronomy, Vol. 3, G. Gontopoulos and G. Gontopoulos, eds. (Dordrecht: Reidel), p. 395.
Wright, N. J., Drake, J. J., Mamajek, E. E., & Henry, G. W. 2011, ApJ, 743, 48
Zhang, J., Zhao, Oswalt, T. D. et al. 2019, ApJ, 887, 84